Materials Research Express

PAPER

Capacitance–conductance characteristics of Au/Ti/Al_2O_3/*n*-GaAs structures with very thin Al_2O_3 interfacial layer

To cite this article: A Turut *et al* 2015 *Mater. Res. Express* **2** 046301

View the article online for updates and enhancements.

Related content

- Influence of Al2O3 barrier on the interfacial electronic structure of Au/Ti/n-GaAs structures
Abdulkerim Karabulut, Hasan Efeoglu and Abdulmecit Turut
- Electrical characteristics of Au/Ti/n-GaAs contacts over a wide measurement temperature range
Necmi Biyikli, Abdulkerim Karabulut, Hasan Efeolu et al.
- Au/n-InP Schottky diodes using an Al2O3 interfacial layer grown by atomic layer deposition
Hogyoung Kim, Min Soo Kim, Seung Yu Yoon et al.

Recent citations

- Investigation of temperature dependent negative capacitance in the forward bias C-V characteristics of (Au/Ti)/Al2O3/n-GaAs Schottky barrier diodes (SBDs)
Ç.. Güçlü *et al*
- Photodiode based on Pb0.9Cd0.1S ternary alloy semiconductor for solar tracking systems
S. Wageh *et al*
- Cadmium Oxide:Titanium Dioxide Composite Based Photosensitive Diode
Abdulkerim Karabulut *et al*

IOP ebooks™

Bringing you innovative digital publishing with leading voices to create your essential collection of books in STEM research.

Start exploring the collection - download the first chapter of every title for free.

This content was downloaded from IP address 139.179.72.98 on 26/11/2018 at 14:57

Materials Research Express

PAPER

RECEIVED
20 November 2014

REVISED
10 February 2015

ACCEPTED FOR PUBLICATION
25 February 2015

PUBLISHED
20 March 2015

Capacitance–conductance characteristics of Au/Ti/Al_2O_3/*n*-GaAs structures with very thin Al_2O_3 interfacial layer

A Turut[1,6], A Karabulut[2], K Ejderha[3] and N Bıyıklı[4,5]

1 Istanbul Medeniyet University, Faculty of Sciences, Engineering Physics Department, TR-34730 Istanbul, Turkey
2 Sinop University, Faculty of Engineering, Department of Electrical and Electronics Engineering, Sinop, Turkey
3 Bingöl University, Faculty of Sciences and Arts, Department of Physics, 12000 Bingöl, Turkey
4 Institute of Materials Science and Nanotechnology, Bilkent University, Bilkent, Ankara 06800, Turkey
5 National Nanotechnology Research Center (UNAM), Bilkent University, Bilkent, Ankara 06800, Turkey
6 Author to whom any correspondence should be addressed.

E-mail: abdulmecit.turut@medeniyet.edu.tr, amecit2002@yahoo.com, akerimkara@gmail.com, kadir2538@gmail.com and biyikli@unam.bilkent.edu.tr

Keywords: high dielectric material, atomic layer dedeposition, MIS devices

Abstract

High-*k* Al_2O_3 with metallic oxide thickness of about 3 nm on *n*-type GaAs substrate has been deposited by the atomic layer deposition (ALD) technique. Thus, it has been formed the Au-Ti/Al_2O_3/*n*-GaAs MIS structures. It has been seen that the MIS structure exhibits excellent capacitance-voltage (*C*–*V*) and current-voltage (*I*–*V*) properties at 300 K. The saturation current of the forward bias and reverse bias *I*–*V* characteristics was the same value. An ideality factor value of 1.10 has been obtained from the forward bias *I*–*V* characteristics. The *C*–*V* characteristics of the structure have shown almost no hysteresis from +3 V to −10 V with frequency as a parameter. The reverse bias *C*–*V* curves have exhibited a behavior without frequency dispersion and almost hysteresis at each frequency from 10 kHz to 1000 kHz.

1. Introduction

Metal/oxide (insulator)/semiconductor field effect transistor (MOSFET) systems are important conventional devices in integrated circuit technology. MOS transistors are also increasingly used in analog applications such as switched capacitor circuits, analog-to-digital converters and filters [1–9]. As mentioned by Wu and colleagues [10], the integrated circuit fabrication based on MOSFET relies on thermally grown amorphous SiO_2 as a gate dielectric, and a stable Si:SiO_2 interface offers many important materials and electrical properties such as the excellent electrical insulation and interfacial bonding properties. However, in order to avoid severe short channel effects, the gate dielectric thickness must also be reduced to the point that leakage current becomes unacceptable. Therefore, the SiO_2 must be replaced with other gate dielectrics [10–24], that is, the reduction of gate dimensions requires decreasing oxide thickness to prevent the short channel effect and therefore the undesirable gate leakage current is substantial and increases exponentially with decreasing thickness. This calls for other dielectrics with much higher dielectric constants, that is, the high-κ metallic gate oxides which allow maintenance of the gate oxide capacitance needed for reducing short channel effects [10–24]. Wu and colleagues have reported [10] that the atomic layer deposition (ALD) method is the most widely used technique in spite of the fact that other methods have also led to attractive results, and that the ALD has improved the interface quality and reduced the defects density in high-κ films. Furthermore, Deposition of the SiO_2 onto GaAs substrate creates a high density of interface states. These facts practically prevent implementation of MOS capacitor with GaAs substrate [1].

We have prepared the MIS (metal/insulator/semiconductor) Au/Ti/Al_2O_3/*n*-GaAs/In. The Al_2O_3 metal oxide layer on the GaAs substrate was formed by ALD method, and the film thickness of the Al_2O_3 layer was about 3 nm. As stated by Pan *et al* [12], the complementary metal oxide semiconductor (MOS) devices require gate oxide of about 1 nm to reduce the gate leakage current and maintain the gate capacitance. This is the reason

© 2015 IOP Publishing Ltd

why we take such a thickness. Thickness of conventional SiO_2 less than 20 Å is inevitable to excessive leakage current due to the occurrence of direct tunneling. Therefore, silicon dioxide has to be substituted by a high dielectric constant material, which provides a physically thicker film for the same electrically equivalent oxide thickness [12]. Au(50 nm)/Ti(10 nm) Schottky contacts have been fabricated on Al_2O_3/*n*-GaAs structure using magnetron dc sputter technique. Au thin films are more often used as a top layer to protect other metallic layers. Al_2O_3 is an attractive candidate for the high-κ material; it has a dielectric constant of 8.6 and a wide bandgap of about 6.6 eV (for the amorphous oxide typical of ALD-grown layers). Titanium is commonly used as a standard gate metal in the fabrication of GaAs field effect transistors (FET) and MESFET since it has good adhesion and is stable against inter-diffusion and compound formation and has good electrical properties at room temperature and elevated temperatures [23, 24].

Moreover, the method used to form the oxide layer in the MOS systems affects device performance and stability and plays an important role in integrated circuits. Furthermore, It has been examined that high-κ metallic gate oxides such as Al_2O_3, Nd_2O_3, Gd_2O_3 and HfO_2 become the potential materials and high dielectric permittivity to replace silicon dioxide SiO_2 [9–12], and ALD technique can be preferred to the other techniques for the deposition of metallic gate oxide Al_2O_3, Nd_2O_3 and Gd_2O_3 due to its unparalleled uniformity and precise thickness control technique. Pan *et al* [12] have reported that TiN/Nd_2O_3/*p*-Si/Al MOS capacitors with film thickness of about 6.5 nm grown by reactive rf sputtering exhibit excellent electrical properties such as high electric breakdown field and being without frequency dispersion and almost hysteresis in capacitance–voltage (*C*–*V*) curves after annealing at 700 °C treatment. Raeissi *et al* [13] have investigated electron capture for insulator/silicon interface states for high-κ dielectrics of Gd_2O_3 grown on silicon wafers by molecular beam epitaxy (MBE) and ALD, and for HfO_2 prepared by reactive sputtering by measuring the frequency dependence of MOS capacitance. Kundu *et al* [14] have fabricated GaAs-based MOS devices with TiO_2 layer having three different thicknesses of 33, 54 and 71 nm of TiO_2 by the sol–gel technique and they have shown that the *C*–*V* characteristics have strongly depended on applied voltage and the interfacial layer thickness and frequency in the frequency range 10 kHz–1 MHz [14].

Long *et al* [16, 17] reported the *C*–*V* measurements of Pd/Al_2O_3/GaN MOS capacitors with the Al_2O_3 layer of approximately 8 nm by ALD, over a temperature range of 77–500 K. They [16, 17] have estimated the interface state density of the wide band gap GaN semiconductor by the limitations of the conductance method in this temperature range, and have described the role of the pyroelectric effect in the interpretation of higher temperature capacitance–voltage data, because GaN-based devices are intended for high temperature applications. Saghrouni *et al* [20, 21] have described the effect of post-deposition annealing on the physical and electrical characteristics of Co/Au/Dy_2O_3/*p*-GaAs device with Dy_2O_3 thickness of 10 nm by electron beam deposition (EBD) under ultra-vacuum. They [20] have found that the annealed device exhibited excellent electrical properties such as small density of interface state and low leakage current, and have studied the ac impedance properties of the structures in a wide frequency range at different bias voltage, and have attributed this phenomenon to a rather crystallized Dy_2O_3 structure and to the reduction of the defects at the oxide/GaAs interface.

It has been stated in the above studies that metal oxides are readily formed by atomic layer deposition. The ALD process for HfO_2 using tetraethylmethylamido hafnium as the metal precursor has resulted in an interfacial layer between the oxide and the semiconductor, in contrast to Al_2O_3 deposition by ALD on surfaces such as GaAs and InGaAs. The initial stages of the Al_2O_3 deposition process by ALD have often been reported to result in the decomposition of native oxides formed on the semiconductor surface, with trimethylaluminium (TMA) as the metal source [17]. Furthermore, Dy_2O_3, like most rare earth oxides, is not usually stoichiometric and often contains significant concentrations of oxygen vacancies which can contribute to leakage current. Thus, it is important to evidence the effects of the native oxide and the different defects such as oxygen vacancies and grain boundaries on the electrical and dielectrical properties of MIS or MOS structures [20, 21]. The opto-electrical characteristics of MIS structures are controlled mainly by its interface properties [1–7, 25–30]. As is well-known, the *C*–*V* plot or admittance value differs significantly from that expected for an ideal MIS diode, and thus the performance of the metal oxide/GaAs-based electronic and optical devices is reduced [1–7, 25–30]. Therefore, studies on interface properties are essential in the understanding of the electrical properties of the MIS structures, and are especially of technological importance for developing GaAs-based devices [25–30].

2. Experimental details

Au/Ti/Al_2O_3/*n*-GaAs MIS structures were fabricated using *n*-type single crystals GaAs wafer with (100) surface orientation, having thickness of 300 μm, 6.8×10^{15} cm^{-3} carrier concentration (N_D) and 1.2 Ω cm resistivity (given by the manufacturer). Before the SBDs fabrication process, the experimental procedure was carried out first as a cleaning procedure, that is: sonicated for two minutes in acetone and two minutes in prophanol,

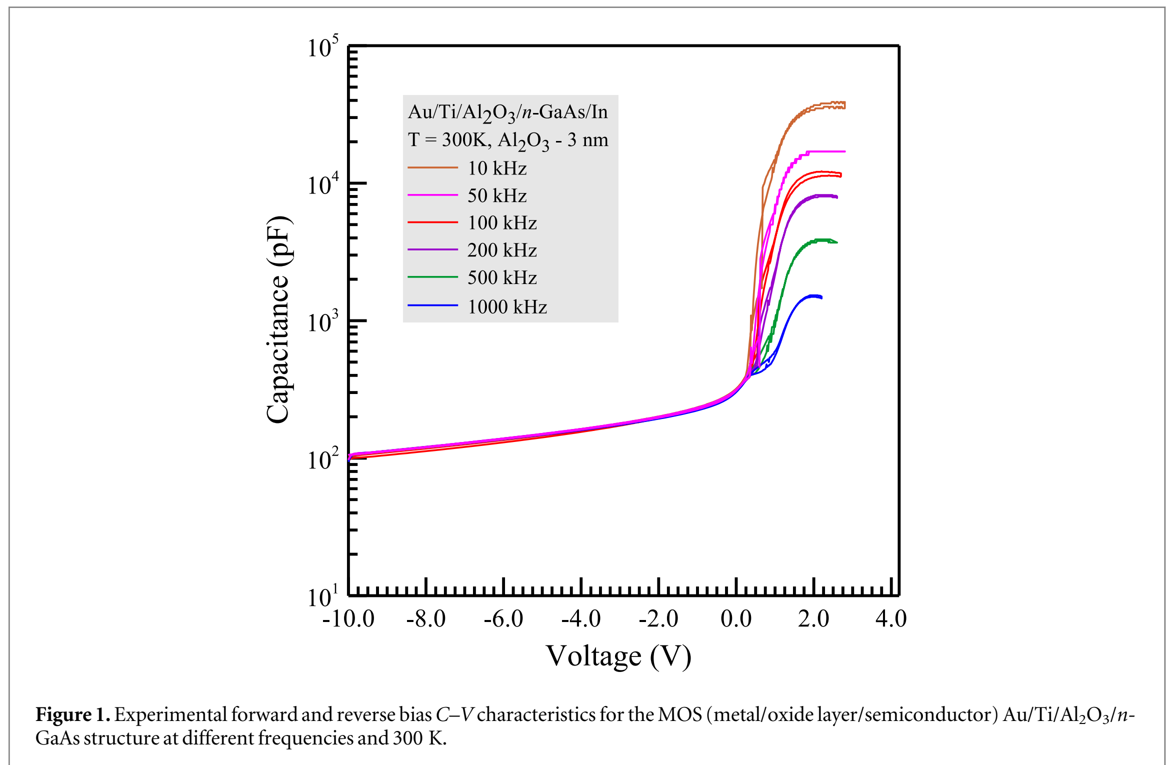

Figure 1. Experimental forward and reverse bias *C–V* characteristics for the MOS (metal/oxide layer/semiconductor) Au/Ti/Al_2O_3/*n*-GaAs structure at different frequencies and 300 K.

respectively; then, rinsed in DI water of resistivity of 18 MΩ cm for an extended time and dried under N_2 flow. After surface cleaning of *n*-GaAs, high purity (99.999%), In with a thickness of about 2000 Å was coated for ohmic contact at a base pressure about 10^{-6} Torr. Low ohmic contact to *n*-GaAs was obtained by annealing at 385 °C for three minutes under dry nitrogen flow. The ALD of Al_2O_3 thin films was carried out in Cambridge Nanotech Savannah 100 reactor. The Al_2O_3 deposition was performed at 200 °C using trimethylaluminum (TMA) (Al precursor), and water (oxygen precursor), for a total of 30 cycles. Standard photolithography technique was used for pattern fabrication on GaAs. An Al_2O_3 interface layer is formed by ALD method and Au (90 nm)/Ti(10 nm) Schottky contacts are made using magnetron dc sputter technique. Finally the photoresist was removed by washing with DI water and then with N_2. The $I(V)$ and $C(V,f) - G(V,f)$ characteristics of the device were measured using a Keithley 487 picoammeter/voltage source and an HP 4192 A LF impedance analyzer, respectively, at room temperature in dark.

3. Results and discussion

Figure 1 shows the experimental forward and reverse bias *C–V* characteristics for the MIS Au/Ti/Al_2O_3/*n*-GaAs structure at different frequencies and 300 K. As mentioned above, the thickness of the interfacial layer Al_2O_3 was about 3 nm. For an MIS diode with *n*-type semiconductor, the curve has an accumulation region of electrons and therefore a high differential capacitance of semiconductor in series with the capacitance of the insulator at positive voltage at the right side. As a result, the total capacitance at the accumulation region is close to the capacitance of the insulator [25–30]. As the positive voltage is reduced sufficiently, a depletion capacitance forms near the semiconductor surface, and the total capacitance decreases because the depletion region acts as a dielectric in series with the interfacial insulator layer [25–30]. As can be seen from figure 1, the hysteresis behavior with a very narrow window was observed for the MIS *C–V* curves at all frequencies. It can be said that the sample has a negligibly thin interfacial-layer thickness. Another possible reason for this behavior is mobile charges in the oxide layer. This relatively smaller hysteresis phenomenon can be ascribed to the trapped charges at defect sites to be passivized due to the Al_2O_3 layer, and to the reduction of interface traps at Al_2O_3 layer and GaAs interface [3, 25–30].

The characteristics parameters of the ideal Schottky diodes can be calculated using the thermionic emission (TE) current expression. The *I–V* equation by the forward bias TE theory is given as follows [28–31]

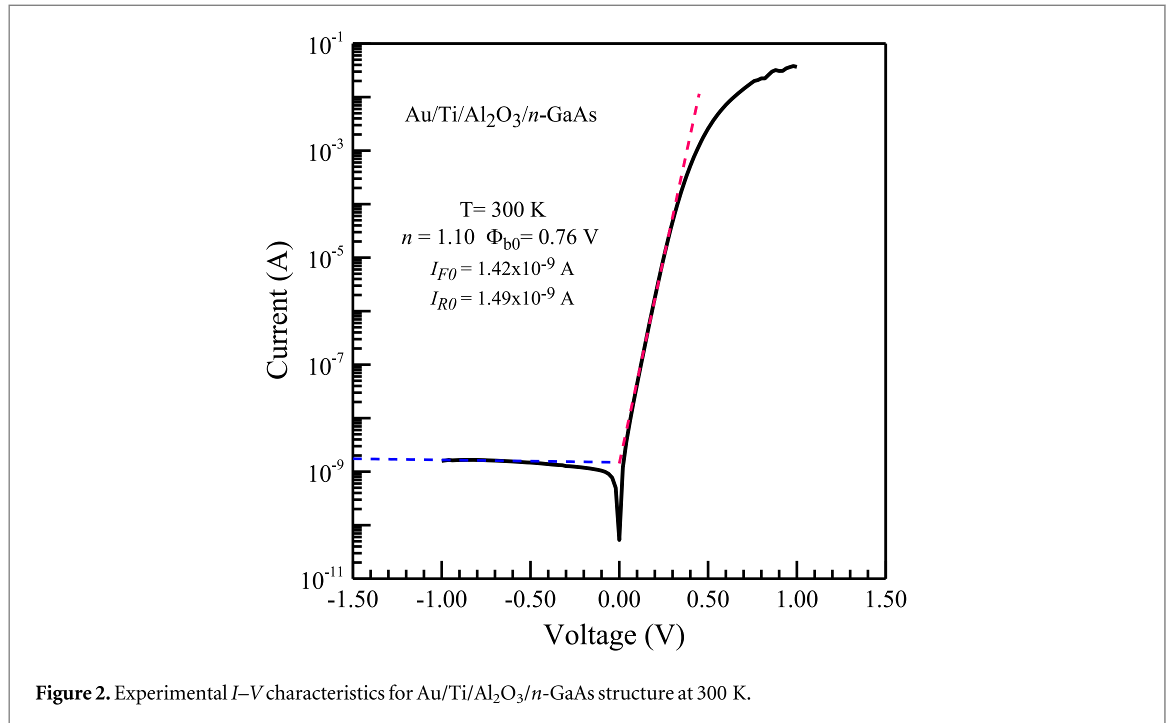

Figure 2. Experimental I–V characteristics for $Au/Ti/Al_2O_3/n$-GaAs structure at 300 K.

$$I = I_0\left[\exp\left(\frac{q\left(V - IR_s\right)}{nkT}\right) - 1\right], \tag{1}$$

Where I_0 is the saturation current

$$I_0 = AA^*T^2\exp\left(-\frac{q\Phi_{b0}}{kT}\right), \tag{2}$$

is the saturation current density, Φ_{b0} and n are the effective barrier height (BH) at zero bias and ideality factor calculated from the intercept and slope of the linear portion of the semi-log forward bias ln I–V characteristics, respectively, A^* is the effective Richardson constant of 8.16 A $(cm^2\ K^2)^{-1}$ for n-type GaAs, A is the diode area. R_s is the series resistance of the neutral region of the semiconductor substrate between the depletion region and ohmic contact. IR_s and $(V–IR_s)$ are the voltage drop across the series resistance and the depletion region, respectively. The series resistance value of the $Au/Ti/Al_2O_3/n$-GaAs MIS diode was calculated as 11.30 Ω from the data of downward curvature region of the forward bias I–V characteristics using Cheung's functions [31]. For values of $q(V–IR)$ greater than 3 kT, the ideality factor is given by

$$n = \frac{q}{kT}\frac{\mathrm{d}V}{\mathrm{d}(\ell nI)}. \tag{3}$$

The value of n indicates the deviation from ideal forward bias characteristics for Schottky diodes. The high values of n can be attributed to effects of the bias voltage drop across the interfacial layer and, therefore, of the bias voltage dependence of the barrier height [32–46].

Figure 2 shows the semi-log reverse and forward I–V curves of the $Au/Ti/Al_2O_3/n$-GaAs MIS diode at 300 K. The experimental values of the BH and ideality factor from the intercept and slope of the linear portion of the forward-bias ln$I$ versus V plot have been calculated as 1.10 and 0.76 eV for 300 K, respectively. The intercepts or the saturation currents at $V = 0$ volts for the reverse bias and forward bias branch correspond to 1.49×10^{-9} A and 1.42×10^{-9} A. These values say that the device shows an excellent rectification or diode behavior. The saturation current values give a value of about 0.76 eV using equation (2). The ideality factor value of 1.10 says that the current flow across the device is dominated by the thermionic emission over the BH because the Al_2O_3 interfacial layer is very thin. As mentioned by Zussman [33], the sputter process relative to the evaporation process can improve the properties of diode due to a process of cleaninig of the surface of the substrate taking place during the sputter deposition as a result of the chemical reactivity of the plasma tail and high energy of the sputtered atoms.

Goksu *et al* [34] used the GaAs semiconductor substrate with the same carrier concentration (7.43×10^{15} cm^{-3}) and fabricated for Ti/n-GaAs diodes without the interfacial layer prepared by magnetron dc sputtering and obtained a BH value of 0.90 eV with an ideality factor 1.02 for this diode at 300 K. Myburg *et al*

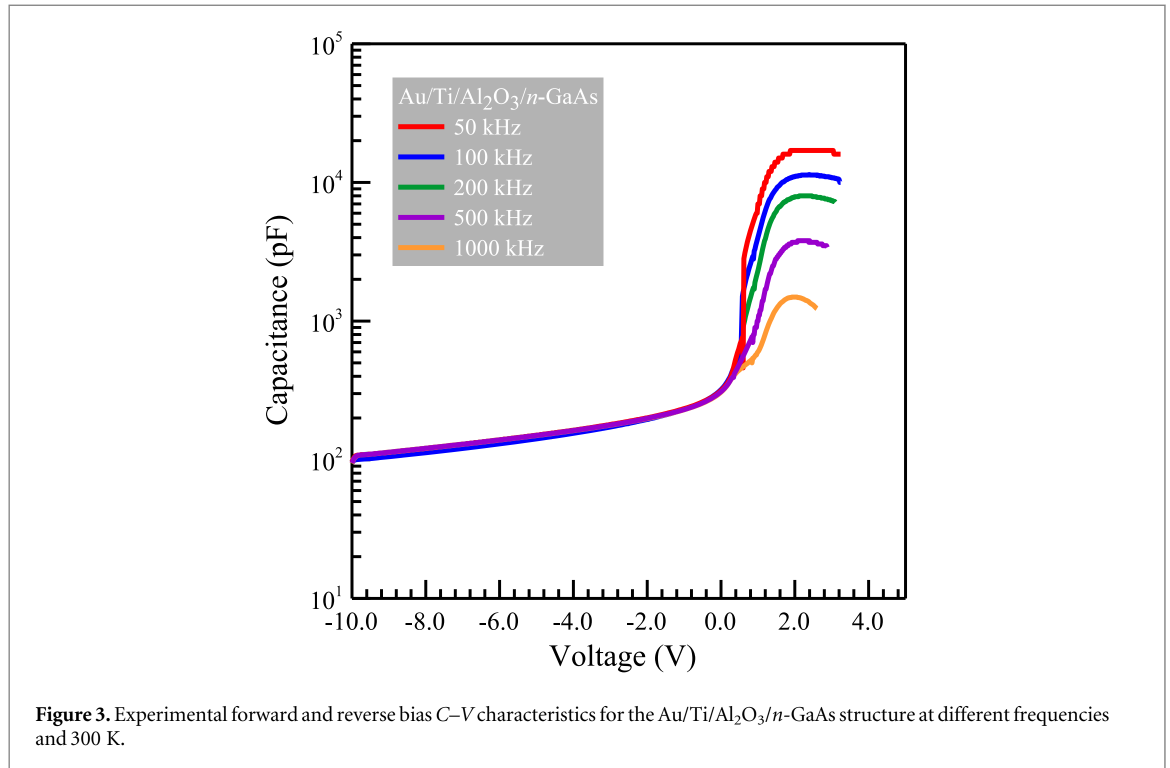

Figure 3. Experimental forward and reverse bias *C–V* characteristics for the Au/Ti/Al_2O_3/*n*-GaAs structure at different frequencies and 300 K.

[35] have fabricated Ti/*n*-GaAs Schottky diodes using *n*-GaAs epilayer layer with a free carrier concentration (Si doped) of 1×10^{16} cm^{-3} grown on n^+-GaAs semiconductor substrate by organometallic vapor phase epitaxy, and they [35] have reported a BH value of about 0.83 eV with an ideality factor of 1.03 for this diode at 300 K. Dio *et al* [36] have measured forward and reverse bias *I–V* characteristics of Au/Ti/*n*-GaAs diodes prepared by ion beam sputtering at different sputtering voltages and currents and they [36] have reported BH values from 0.79 to 0.83 eV and ideality factor from 1.03 to1.10 for these diodes at 300 K. Ayyildiz and Turut [37] have given a BH value of about 0.64 eV with an ideality factor of 1.08 from forward bias *I–V* characteristics (300 K) of Ti/*n*-GaAs diodes prepared by evaporation of Ti. Cola *et al* [38] have reported BH values from 0.828 to 0.854 eV and ideality factor values from 1.01 to1.08 (300 K) from forward bias *I–V* characteristics of Au/Ti/*n*-GaAs diodes prepared by ion beam sputtering at different sputtering voltages and currents. As can be seen, the value of 0.76 eV we have found for the Au/Ti/Al_2O_3/*n*-GaAs MIS diode prepared by magnetron dc sputtering differs from the results in the literature given above. The reason for difference can be due to the presence of the Al_2O_3 layer at the Au/Ti and *n*-GaAs interface. Therefore, it can be said that the Al_2O_3 layer can be used to realize the barrier height modification in the Schottky diodes.

Let us now consider the MIS structure with the interfacial layer for the *I–V* characteristics. Kundu *et al* [14] have found ideality factor values of 1.10, 1.13 and 1.15 for *n*-GaN based MOS structures with TiO_2 thicknesses of 33, 54 and 71 nm prepared by the sol–gel technique, respectively, for which their MOS structures [14] have given the non-saturated reverse bias *I–V* curves. Reddy *et al* [22] have reported that the BH values of the Au/ $BaTiO_3$/ *n*-GaN structure with values of 0.87 eV (*I–V*) and 1.02 eV (*C–V*) increases compared with those of the Au/*n*-GaN MS structure with 0.73 eV (*I–V*) and 0.96 eV (*C–V*). They [22] have formed $BaTiO_3$ thin films of about 60 nm thick on the surface of the cleaned *n*-GaN substrates by spin coating.

Figure 3 shows the experimental forward (0.0 V to 3.2 V) and reverse bias (0.0 V to −10 V) *C–V* characteristics for the Au/Ti/Al_2O_3/*n*-GaAs MIS structure at different frequencies and 300 K. As can be seen from figure 3, the capacitance curve saturates in the high forward bias voltage. These saturation regions are known as the accumulation region giving the capacitance of the interfacial layer (Al_2O_3) C_{ox} and thus its thickness. The value of C_{ox} determined from the accumulation region in figure 3 decreases with increasing frequency. This value is 17 000 pF at 50 kHz and 1350 pF at 1000 kHz. The values of C_{ox} for each frequency are given in table 1. Furthermore, the capacitance of the interfacial layer per area unit in a MIS diode is given by

$$C_{ox} = \frac{\varepsilon_{in}\varepsilon_0 A}{d}, \tag{4}$$

where ε in and d are the permittivity of interfacial layer and its thickness, respectively, ε_0 is the permittivity of free space and A is the area of diode. A value of 4.11 nm for the thickness of the interfacial layer Al_2O_3 was obtained using C_{ox} value at 50 kHz in equation (4). This value is in close agreement with the Al_2O_3 layer thickness of

Table 1. Experimental values from the reverse and forward bias characteristics for the Au/Ti/Al_2O_3/n-GaAs MIS structure at different frequencies and 300 K.

				0.0 Volts		−10 Volts	
f(kHz)	C_{ox} (pF)	ε_{in}	R_s (Ω)	G (F s^{-1})	Z (Ω)	G (F s^{-1})	Z (Ω)
50	17 000	7.97	4.99	1.0×10^{-6}	10 101.00	1.0×10^{-7}	32 362.46
100	11 000	4.70	5.00	2.2×10^{-6}	4972.65	2.0×10^{-7}	16 638.94
200	7200	3.38	4.99	5.1×10^{-6}	2554.28	3.0×10^{-7}	8143.32
500	3800	1.78	4.99	1.5×10^{-5}	1031.57	1.3×10^{-7}	3306.88
1000	1350	0.64	4.99	3.2×10^{-5}	518.94	3.6×10^{-7}	1667.78

3.0 nm formed on the GaAs wafer by ALD method. As mentioned above, the decrease in the capacitance value with increasing frequency at a given bias voltage in the plots can be attributed to the decrease of the dielectric constant value of the interfacial layer Al_2O_3 with increasing frequency. However, this is attributed to the fact that the interface state charges cannot follow the ac signal at sufficiently high frequencies, or increase in the capacitance with decreasing frequency is ascribed to the contribution of the interface charges in the interface states [25–30, 40–62]. The decrease in capacitance value can be also due to the series resistance of the Al_2O_3 layer plus the neutral region of the semiconductor substrate. The series resistance of the neutral region of the semiconductor substrate between the depletion region and the back contact is the real part of the impedance. A thicker interfacial layer may cause larger series resistance. The series resistance value at each frequency can be large enough to affect the device capacitance. It can cause a serious error in the extraction of the interfacial properties, that is, the series resistance completely masks interface trap loss, and especially the equivalent parallel conductance is much more sensitive to the series resistance than capacitance. Thus, it can be said that the correction for the series resistance is particularly important in conductance measurements. Furthermore, the values of dielectric loss tangent and ac conductivity strongly depend on applied voltage and the thickness of the interfacial oxide layer [1–3, 14–23].

Moreover, the low value of dielectric constant could be due to the formation of the native oxides related to Ga and As during devices fabrication processes. In addition, the diffusion of Ga and As atoms into the high-κ can exacerbate the interface quality between the high-κ dielectric and GaAs [9, 12, 20–22]. The dielectric constant expression of the interfacial layer is given by

$$\varepsilon_{in} = \frac{C_{ox} d}{\varepsilon_0 A} = \frac{C_{ox}}{C_0}, \tag{5}$$

where C_0 is capacitance of an empty capacitor, d is the thickness of interfacial layer Al_2O_3. The dielectric constant value of the Al_2O_3 layer was obtained using the C_{ox} value from the accumulation region at each frequency in equation (5). The dielectric constant decreases with increase in frequency, as can be seen in table 1.

Again, as can be seen from figure 3, the capacitance of the device is independent of the measurement frequency under the reverse bias (0.0 V to −10 V), that is, there is almost no frequency dispersion in the reverse bias. Figure 4 shows the phase angle versus bias voltage curves for the device at different frequencies at the room temperature. The phase angle is always 90° from −10 V to 0.0 V in the reverse bias branch, and it suddenly decreases at 0.0 V and then approaches 0° from 0.0 V to 4.0 V in the forward branch. The case clearly indicates that the diode behaves more capacitively at the reverse bias region rather than the forward bias region [51]. Figure 5 shows the impedance modulus (Z) versus bias voltage curves for the device at different frequencies at room temperature. It has been observed that the impedance modulus depends on frequency and bias at the reverse bias while it is frequency-independent and strongly bias-dependent for the forward bias, that is, the impedance modulus decreases with increasing frequency at a given reverse bias, and decreases with increasing bias independently of frequency by coinciding (overlap) with each other from about 0.6 V to 4.0 V at the forward bias. Figure 6 shows the conductance (G) versus bias voltage curves for the device at different frequencies at room temperature. The conductance is frequency-dependent and bias-dependent for the reverse bias while it is frequency-independent and strongly bias-dependent at the forward bias, that is, the conductance increases with decreasing frequency at a given reverse bias, and increases with increasing bias as independent of frequency by coinciding with each other from about 0.0 V to 4.0 V for the forward bias. The impedance modulus and conductance values at 0.0 V and −10 V are given in table 1 for different frequencies. It can be clearly seen from values at 0.0 V and −10 V in table 1 how the impedance modulus and conductance values change depending on frequency and bias voltage. This behavior indicates that the device has the same series resistance value at a given forward bias voltage for all frequencies, as can be seen in table 1, thus the conductance data confirm the impedance modulus data in the forward and reverse bias regime. The series resistance expression of the MIS devices is given by [3]

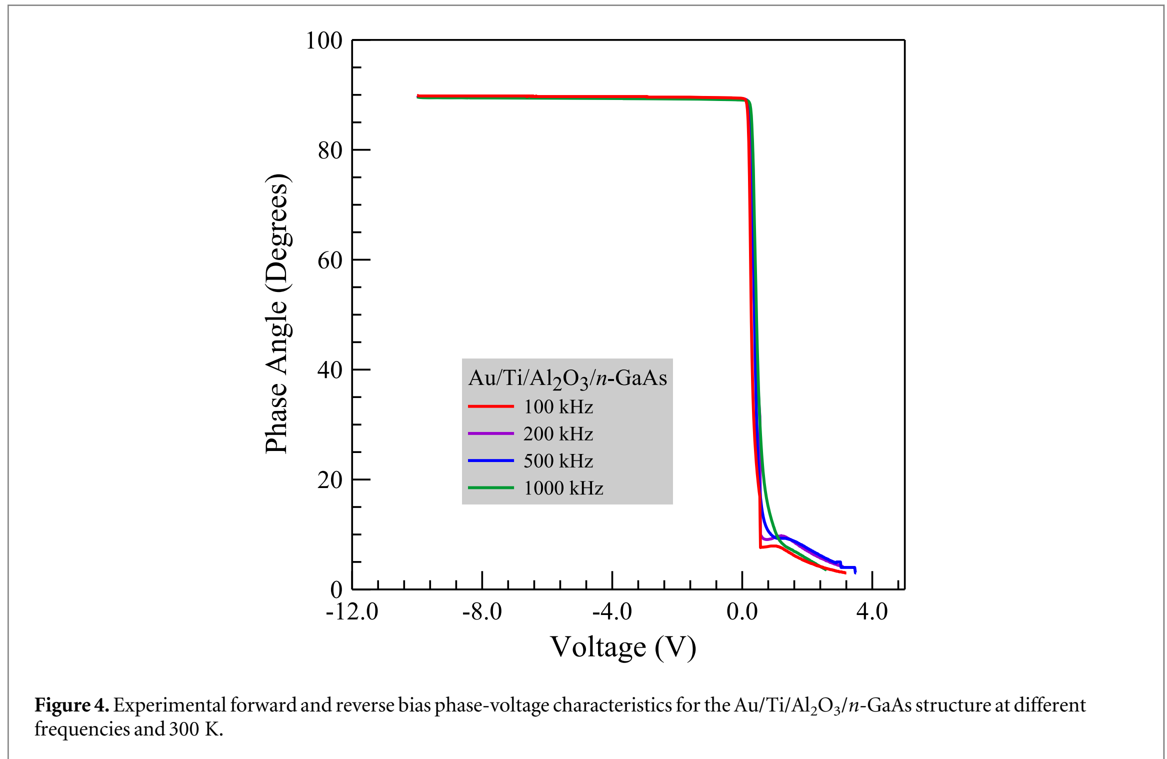

Figure 4. Experimental forward and reverse bias phase-voltage characteristics for the Au/Ti/Al_2O_3/*n*-GaAs structure at different frequencies and 300 K.

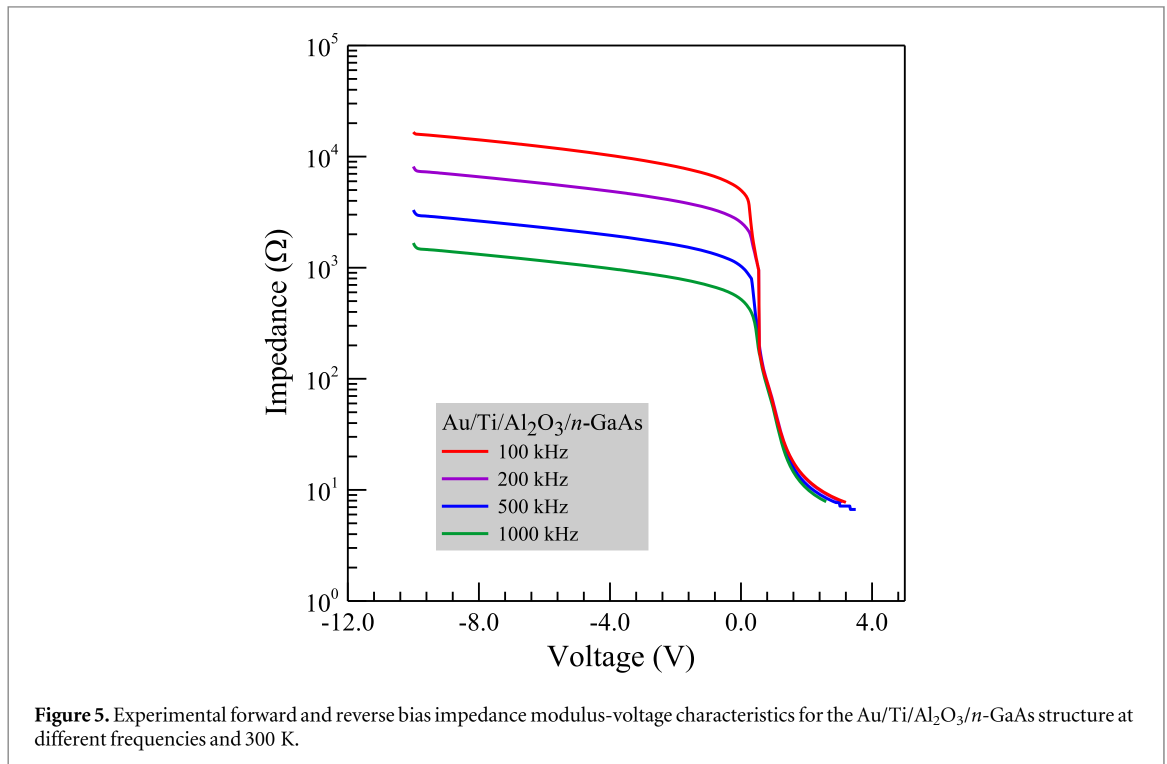

Figure 5. Experimental forward and reverse bias impedance modulus-voltage characteristics for the Au/Ti/Al_2O_3/*n*-GaAs structure at different frequencies and 300 K.

$$R_s = \frac{G_m}{G_m^2 + w^2 C_m^2}, \quad (6)$$

where G_m and C_m are the experimental conductance and capacitance values from the strong accumulation region for each frequency. The series resistance of the device is obtained using G_m and C_m values given in table 1 in equation (6). As can be seen in table 1, the series resistance value of the device for each frequency approximately equals 5 Ω.

In *C–V* measurements, the charges at the interface states cannot follow the ac signal at very high frequencies [40–62], and the equivalent circuit of device will be just the interfacial layer and depletion (the space charge region) capacitance in series. At very high frequency, the total capacitance, *C*, per area unit of MIS diode is a

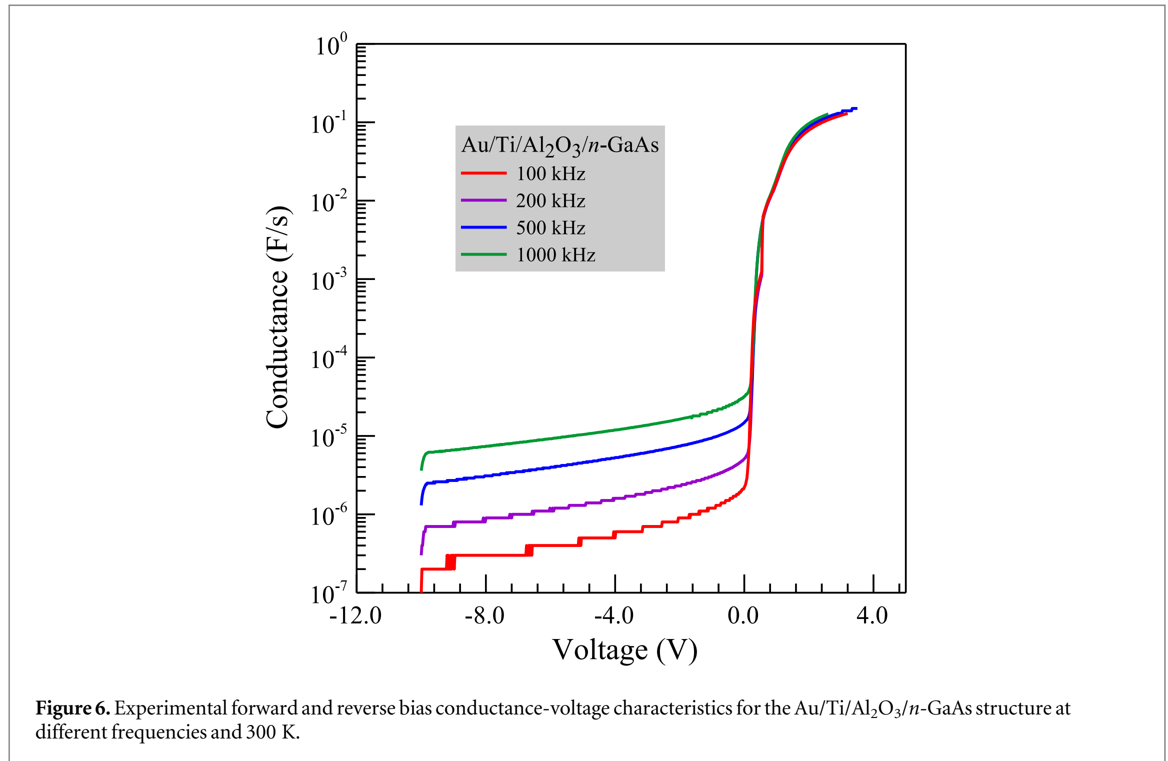

Figure 6. Experimental forward and reverse bias conductance-voltage characteristics for the Au/Ti/Al_2O_3/n-GaAs structure at different frequencies and 300 K.

series combination of the depletion capacitance of the semiconductor C_D and the capacitance of the interfacial layer C_{ox}, and thus the total capacitance C is represented by [27–30, 45–50]

$$\frac{1}{C} = \frac{1}{C_D} + \frac{1}{C_{ox}}, \tag{7}$$

C_{ox} is the capacitance of the interfacial layer and corresponds to the maximum capacitance of the MIS diode, and C_D depends on the bias voltage. It has been stated above that the C–V curve has an accumulation region at positive voltage at the right side which gives the capacitance of the insulator [27–30], as can be seen from figures 1 or 3. A depletion capacitance forms near the semiconductor surface from the positive voltage to negative, or as the positive voltage is reduced sufficiently, and the total capacitance decreases because the depletion region acts in series with the interfacial insulator layer [27–30]. Thus, in this case, it can be said that the negative voltage region in figures 1 and 3 corresponds to the deep depletion condition [3, 27–30]; the depletion capacitance C_D can approximately be given by [27–30, 46–50]

$$\frac{1}{C_D^2} = \frac{2\left(\Phi_{b0}^{CV} - V - V_n\right)}{q\varepsilon_s N_d A^2}, \tag{8}$$

where V_n is the potential difference between the Fermi level and the conduction band minimum in the neutral region of n-type semiconductor, $(\Phi_{b0}^{CV} - V_n) = V_{D0}$ is the diffusion potential at the zero bias, N_d is the doping concentration of the n-type semiconductor, ε_s is the permittivity of the semiconductor, q is the electronic charge and A is the diode area. Figure 7 shows the experimental reverse bias C^{-2}–V characteristics for the Au/Ti/Al_2O_3/n-GaAs structure at various frequencies and 300 K. As can be seen from equation (7), the C^{-2} versus V plot is a straight line whose intercept with V axis gives the value of $V_0 = V_{D0}$, and the slope gives the value of N_d. N_d can be given as follows:

$$N_d = \frac{2}{q\varepsilon_s A^2}\frac{dV}{d\left(C^{-2}\right)}. \tag{9}$$

The values of $V_0 = 1.86$ V, $V_n = 0.083$ V, $\Phi_{b0}^{CV} = 1.92$ V and $N_d = 1.61 \times 10^{16}$ cm^{-3} were obtained from the experimental reverse bias C^{-2}–V plot. As can be seen from the obtained barrier height values, there is an appreciable difference between the barrier height values obtained I–V and C–V characteristics. That is, the barrier height value from I–V characteristics is much lower than that from the C–V characteristics. Likewise, the experimental carrier concentration value of $N_d = 1.61 \times 10^{16}$ cm^{-3} from C–V characteristics is significantly higher than the value of 7.43×10^{15} cm^{-3} given for the n-GaAs used this study. The barrier height and carrier concentration change in the MS contacts with the interfacial layer depends on the position of the Fermi level and interface-state density. The change in positive or negative interface charge will affect the depletion layer of the

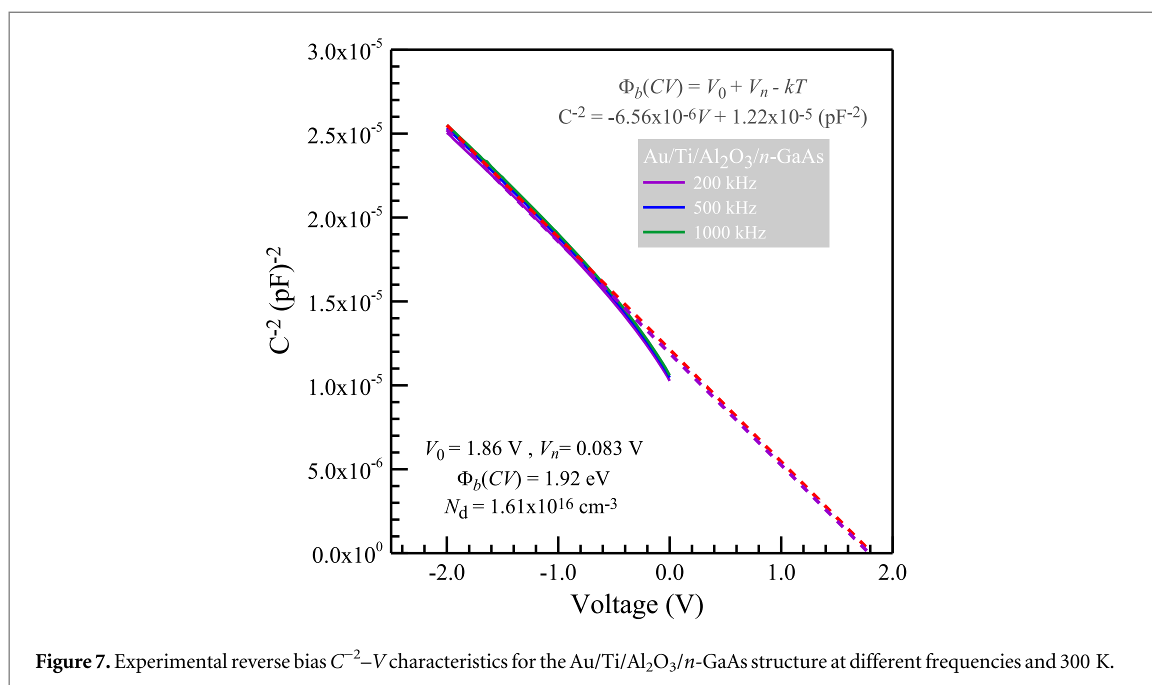

Figure 7. Experimental reverse bias C^{-2}–V characteristics for the Au/Ti/Al_2O_3/n-GaAs structure at different frequencies and 300 K.

semiconductor, and therefore the Fermi-level position. In the absence of the interface states, the negative charge on the metal surface must be equal to the positive space charge due to the neutrality condition. The increase in the barrier height and carrier concentration is evidence for the presence of the negative interface charge, and thus for the positive space charge increase due to the neutrality condition [30, 55, 56].

4. Conclusion

It has been seen that the MIS structure with a high-κ the Al_2O_3 gate dielectric that we have grown by the ALD on the n-GaAs substrate exhibits excellent electrical properties, that is, the structure has shown almost no hysteresis over the whole bias region and no frequency dispersion in the reverse bias C–V curves for all frequencies. This film appears to be a very promising high-κ gate dielectric with very thin film of about 3 nm for future ultra-large scale integration devices.

Acknowledgments

This work was performed in part at the UNAM-Institute of Materials Science and Nanotechnology which is supported by the State Planning Organization of Turkey through the National Nanotechnology Research Center Project. The measurements were made at Department of Physics, Faculty of Sciences and Arts, Bingöl University, Turkey.

References

[1] Colinge C P and Colinge C A 2002 *Physics of Semiconductor Devices* (Dordrecht: Kluwer)
[2] Dimitrijev S 2012 *Prenciples of Semiconductor Devices* (Oxford: Oxford University press)
[3] Nicollian E H and Brews J R 1982 *MOS (Metal Oxide Semiconductor) Physics and Technology* Bell Laboratories, Murray Hill (New York: Wiley)
[4] Oh S-K, Shin H-S, Li M, Lee H, Lee G-W and Lee H-D 2014 *Japan. J. Appl. Phys.* **53** 08NE05
[5] Pakma O, Serin N, Serin T and Altındal Ş 2008 *J. Appl. Phys.* **104** 014501
[6] Caldıran Z, Deniz A R, Coskun F M, Aydogan S, Yesildag A and Ekinci D 2014 *J. Alloys Compd.* **584** 652–7
[7] Ozdemir A F, Aydin S G, Aldemir D A and Gursoy S S 2011 *Synth. Met.* **161** 692–7
[8] Kaya A, Zeyrek S, San S E and Altındal Ş 2014 *Chin. Phys.* B **23** 018506
[9] Mönch W 2005 *Appl. Phys. Lett.* **86** 122101
[10] Wu M, Alivov Y I and Morkoc H 2008 *J. Mater. Sci., Mater. Electron.* **19** 915–51
[11] Ye P D *et al* 2003 *IEEE Electron Device Lett.* **24** 209
[12] Pan T-M, Lee J-D, Shu W-H and Chen T-T 2006 *Appl. Phys. Lett.* **89** 232908
[13] Raeissi B, Piscator J, Engström O, Hall S, Buiu O, Lemme M C, Gottlob H D B, Hurley P K, Cherkaoui K and Osten H J 2008 *Solid-State Electron.* **52** 1274–9
[14] Kundu S, Roy S K and Banerji P 2011 *J. Phys. D: Appl. Phys.* **44** 155104
[15] Kınacı B, Cetin S S, Bengi A and Ozcelik S 2012 *Mater. Sci. Semicond. Process.* **15** 531–5

[16] Long R D, Hazeghi A, Gunji M, Nishi Y and McIntyre P C 2012 *Appl. Phys. Lett.* **101** 241606
[17] Long R D and McIntyre P C 2012 *Materials* **5** 1297–335
[18] Bioki H A 2013 *Eur. Phys. J. Appl. Phys.* **62** 20201
[19] Gupta R K and Yakuphanoglu F 2013 *Microelectron. Eng.* **105** 13–7
[20] Saghrouni H, Jomni S, Belgacem W, Hamdaoui N and Beji L 2014 *Physica* B **444** 58–64
[21] Saghrouni H, Jomni S, Belgacem W, Elghoul N and Beji L 2015 *Mater. Sci. Semicond. Process.* **29** 307–14
[22] Reddy V R, Manjunath V, Janardhanam V, Kil Y-H and Choi C-J 2014 *J. Electron. Mater.* **43** 3499
[23] Cherif A, Jomni S, Belgacem W, Elghoul N, Khirouni K and Beji L 2015 *Mater. Sci. Semicond. Process.* **29** 143–9
[24] Aksoy S and Caglar Y 2014 *J. Alloys Compd.* **613** 330–7
[25] Mir F A, Rehman S, Mir T A, Asokan K and Khan S H 2014 *Appl. Phys.* A **116** 1017–23
[26] Selcuk A B, Ocak S B, Aras F G and Orhan E O 2014 *J. Electron. Mater.* **43** 3263–9
[27] Saglam M, Türüt A, Nuhoglu Ç, Efeoglu H, Kılıçoglu T and Ebeoglu M A 1997 *Appl. Phys.* A **65** 33–7
[28] Sze S M 1981 *Physics of Semiconductor Devices* 2nd edn (New York: Wiley)
[29] Neamen D A 1992 *Semiconductor Physics and Devices* (Boston: Irwin)
[30] Rhoderick E H and Williams R H 1988 *Metal-Semiconductor Contacts* 2nd edn (Oxford: Clarendon)
[31] Cheung S K and Cheung N W 1986 *Appl. Phys. Lett.* **49** 85
[32] Karataş Ş, Altındal Ş and Çakar M 2005 *Physica* B **357** 386–97
[33] Zussman A 1986 *J. Appl. Phys.* **59** 3894–900
[34] Goksu T, Yıldırım N, Korkut H, Ozdemir A F, Turut A and Kokce A 2010 *Microelectron. Eng.* **87** 1781–4
[35] Myburg G, Auret F D, Meyer W E, Louw C W and van Staden M J 1998 *Thin Solid Films* **325** 181–6
[36] Dio M D, Cola A, Lupo M G and Vasanelli L 1995 *Solid-State Electron.* **38** 1923–8
[37] Ayyildiz E and Turut A 1999 *Solid-State Electron.* **43** 521–7
[38] Cola A, Lupo M G, Vasanelli L and Valentini A 1992 *J. Appl. Phys.* **71** 4966–70
[39] Mönch W 2008 *Appl. Phys. Lett.* **93** 172118
[40] Turut A, Sağlam M, Efeoğlu H, Yalcin N, Yildirim M and Abay B 1995 *Physica* B **205** 41–50
[41] Bestas A N, Yazıcı S, Aktas F and Abay B 2014 *Appl. Surf. Sci.* **318** 280–4
[42] Guzeldir B, Sağlam M, Ates A and Turut A 2015 *J. Alloys Compd.* **627** 200–5
[43] Doğan H and Elagöz S 2014 *Physica* E **63** 186–92
[44] Tombak A, Ocak Y S, Genişel M F and Kilicoglu T 2014 *Mater. Sci. Semicond. Process* **28** 98–102
[45] Doğan H, Yıldırım N, Orak İ, Elagöz S and Turut A 2015 *Physica* B **457** 48–53
[46] Rhoderick E H 1970 *J. Phys. D: Appl. Phys.* **3** 1153
[47] Chattopadhyay P and Raychaudhri B 1993 *Solid-State Electron.* **36** 605–10
[48] Ateş A, Güzeldir B and Sağlam M 2011 *Mater. Sci. Semicond. Process.* **14** 28–36
[49] Fonash S J 1983 *J. Appl. Phys.* **54** 1966
[50] Aydogan S, Saglam M and Turut A 2012 *Microelectron. Reliab.* **52** 1362–6
[51] Kim C H, Yaghmazadeh O, Tondelier D, Jeong Y B, Bonnassieux Y and Horowitz G 2011 *J. Appl. Phys.* **109** 083710
[52] Korucu D, Duman S and Turut A 2015 *Mater. Sci. Semicond. Process.* **30** 393–9
[53] Sellai A, Mamor M and Al-Harthi S 2007 *Surf. Rev. Lett.* **14** 765–8
[54] Tuğluoğlu N, Yüksel Ö F, Karadeniz S and Şafak H 2013 *Mater. Sci. Semicond. Process.* **16** 786–91
[55] Biber M and Turut A 2002 *J. Electron. Mater.* **31** 1362
[56] Mönch W 1995 *Semiconductor Surfaces and Interfaces* 2nd edn (Berlin: Springer) pp 75–84 364 and 382–387
[57] Gullu O, Cankaya M, Bibe M and Turut A 2008 *J. Phys.: Condens. Matter* **20** 215210
[58] Gunduz B, Yahia I S and Yakuphanoglu F 2012 *Microelectron. Eng.* **98** 41–57
[59] Ozdemir A, Gok A and Turut A 2007 *Thin Slid Films* **515** 7253–8
[60] Duman S, Ozcelik F S, Gurbulak B, Korucu D, Baris O and Turgut G 2014 *Mater. Sci. Semicond. Process.* **28** 20–5
[61] Asar Y S, Asar T, Altındal S and Ozcelik S 2015 *J. Alloys Compd.* **628** 442
[62] Cakıcı T, Saglam M and Güzeldir B 2015 *Mater. Sci. Eng.* B **193** 61